Small-Angle X-ray and Neutron Scattering from Dilute Solutions of Cesium Perfluorooctanoate. Micellar Growth along Two Dimensions

Hiroshi Iijima and Tadashi Kato*

Department of Chemistry, Faculty of Science, Tokyo Metropolitan University, Minamiohsawa, Hachioji, Tokyo 192-03, Japan

Hirohisa Yoshida

Department of Industrial Chemistry, Faculty of Engineering, Tokyo Metropolitan University, Minamiohsawa, Hachioji, Tokyo 192-03, Japan

Masayuki Imai

Institute for Solid State Physics, University of Tokyo, Tokai, Ibaraki 319-11, Japan

Received: September 16, 1997

Small-angle X-ray and neutron scattering (SAXS and SANS, respectively) have been measured in H_2O solutions of cesium perfluorooctanoate (CsPFO) in the concentration range 0.065−0.5 M (much lower than the boundary between isotropic and discotic nematic phases). For 0.1 and 0.3 M solutions, SANS has been measured for various D_2O/H_2O mixed solvents. The data have been analyzed with a double-layered ellipsoid form factor combined with the rescaled mean spherical approximation for the intermicellar structure factor. The scattering curves can be fitted well with both prolate and oblate ellipsoid models. However, the semiminor axis of micellar core, R_c, obtained for the prolate ellipsoid (15.3 Å) is much longer than the extended length of the fluorocarbon chain (12.6 Å) which is close to the R_c obtained for the oblate ellipsoid (13.0 Å). As the surfactant concentration increases, both the aggregation number and the degree of counterion binding increase. These results suggest micellar growth along two dimensions.

Introduction

It is well-known that micelles grow if required conditions (surfactant concentration, temperature, concentration of added salt, and so on) are satisfied. Under the restriction that all the head groups are exposed to water and that there is no space that is not filled with hydrophobic chains in a micellar core, micelles grow along one dimension (to rod) or two dimensions (to disk).[1] Based on thermodynamic arguments, however, it was shown that surfactants would assemble spontaneously not into finite aggregates but into infinite bilayers in the case of bidimensional growth.[1,2] To the authors' knowledge, in fact, there has been no report showing existence of bidimensional aggregates based on small-angle neutron or X-ray scattering (SANS and SAXS, respectively). Exceptional is a SANS study on mixed short-chain lecithin/long-chain lecithin aggregates by Lin *et al.*[3] In this case, however, the short-chain lecithin molecules may be partially localized in a thin layer covering the edge of the disk and so play an important role in stabilization of the disklike micelle.

On the other hand, Boden, Holmes, and their co-workers[4−13] found that a discotic nematic phase is formed in aqueous solutions of cesium perfluorooctanoate (CsPFO). This is the first report showing that the nematic phase can be formed even in a *binary* (surfactant−water) system. They reported also that there is only small discontinuity in the aggregation number at the isotropic to nematic transition, suggesting the existence of disklike micelles even in the isotropic phase.[6−8] When they obtained the aggregation number in the isotropic phase, however, they assumed that the observed SAXS peak corresponds to the scattering from the (111) planes of a fcc lattice. As there is no evidence supporting this assumption even in the concentrated region, it is still uncertain whether two dimensional micellar growth occurs or not in the isotropic phase.

In the present study, we have tried to elucidate this problem by analyzing curve profiles of SAXS and SANS in the isotropic phase of the CsPFO−water system in the concentration range 0.065−0.5 M at 30 °C. Preliminary results have been already reported elsewhere.[9]

Experimental Section

Materials. CsPFO was prepared by neutralizing perfluorooctanoic acid with cesium hydroxide in acetone. The salts obtained were purified by recrystallization from mixed solvent of hexane and ethanol (1:1) and dried under vacuum. Water (H_2O) was passed through a Mill-Q Labo purification system (Millipore) after distillation. Deuterium oxide was purchased from ISOTEC, Inc. (99.9%). By measuring ^{19}F and ^{133}Cs NMR chemical shifts, the critical micelle concentration (cmc) was determined to be 0.024 mol $kg^{-1} \cong 0.026$ M in D_2O solutions at 30 °C[15] which is equal to the published data in H_2O solutions at 25 °C.[16]

Small-Angle Scattering. Measurements of SANS were carried out using the SANS-U at Institute for Solid State Physics of University of Tokyo, Tokai. The sample-to-detector distance was chosen to be 2 m for all runs. The momentum transfer

* Corresponding author. Phone: +81-426-77-2528. Fax: +81-426-77-2525. E-mail: kato-tadashi@c.metro-u.ac.jp.

S1089-5647(97)03048-4 CCC: $15.00
Published on Web 01/15/1998

was $0.015 < q < 0.15$ Å^{-1} ($q = (4\pi/\lambda) \sin\theta$, where 2θ is the scattering angle and $\lambda = 7.0$ Å is the neutron wavelength). The wavelength resolution, $\Delta\lambda/\lambda$, is 0.1. The samples were filled in a rectangular quartz cell with an inner thickness of 1 mm.

SAXS experiments were performed using SAXS' optics installed at the BL-10C beam line at the Photon Factory of the National Laboratory for High Energy Physics, Tsukuba. The X-ray wavelength and the sample-to-detector distance were 1.49 Å and 84 cm, respectively, corresponding to the momentum transfer of 0.04 Å$^{-1} < q < 0.35$ Å^{-1}. We used a sample cell made of copper with Mylar windows (thickness = 1 mm) whose temperature was controlled by using the DTA/SAXS instrument reported before.[17]

All the measurements were performed at 30 °C. The observed intensities were corrected for transmission and subtracted by a blank measurement with an empty cell. Absolute cross sections, *I(q)*, for SANS were obtained from calculations based on known scattering from pure H_2O. For the SAXS measurements, the sample thickness could not be kept constant due to the deformation of the Mylar windows. So we used the scattering intensities at $q > 0.25$ Å^{-1} as the standard because they are almost independent of the scattering angle and can be regarded as the scattering intensities from pure solvent, H_2O. However, the signal-to-noise ratio for $q > 0.25$ Å^{-1} is not so good as for the lower q range, which may lead to large errors in the accuracy of the absolute cross sections (see later).

Analysis of Data. The observed scattering intensity curves were analyzed by the following procedure. For monodispersed system of ellipsoidal micelles, the scattering intensity can be expressed as[18,19]

$$I(q) = AN_p[\langle F(q)^2\rangle + \langle F(q)\rangle^2(S(q) - 1)] \quad (1)$$

where N_p is the number density of micelles depending on the surfactant concentration and the aggregation number of micelles (m). *F(q)* is the single particle form factor for an ellipsoidal fluorocarbon core plus hydrated Stern layer given by

$$\langle F(q)^2\rangle \equiv \int_0^1 |F(q,x)|^2\, dx \quad (2)$$

$$\langle F(q)\rangle^2 \equiv |\int_0^1 F(q,x)\, dx|^2 \quad (3)$$

$$F(q,x) = (B_c - B_s)V_c[3j(u_c)/u_c] + (B_s - B_w)V[3j(u)/u] \quad (4)$$

$$u_c \equiv qR_c[a_c^2x^2 + (1 - x^2)]^{1/2}, \quad \text{for prolate} \quad (5a)$$

$$u_c \equiv qR_c[a_c^2(1 - x^2) + x^2]^{1/2}, \quad \text{for oblate} \quad (5b)$$

$$u \equiv qR[a^2x^2 + (1 - x^2)]^{1/2}, \quad \text{for prolate} \quad (6a)$$

$$u \equiv qR[a^2(1 - x^2) + x^2]^{1/2}, \quad \text{for oblate} \quad (6b)$$

$$V_c \equiv m\nu_c \quad (7)$$

$$V \equiv m(\nu_c + \nu_s) \quad (8)$$

where B_c, B_s, and B_w are the scattering length densities of the micellar core, micellar shell, and solvent, respectively, determined from the sum of the coherent neutron scattering lengths, b_{coh}, for SANS or the number of electrons (Z) for SAXS divided by the sum of the volumes (see Table 1), j is the first-order spherical Bessel function, R_c and R are the semiminor axes of the micellar core and whole micelle, respectively, ν_c and ν_s are volumes per surfactant molecule in the micellar core and shell, respectively, and a_c and a are the axial ratios of the micellar core and whole micelle, respectively. B_w includes contributions of surfactant monomers (the concentration of which is set equal to the cmc[23]) and free counterions. On the other hand, B_s and ν_s depend on the number of water molecules attached to a polar head group (H_1) and a counterion (H_2). As H_1 and H_2 can not be determined independently, we chose a hydration number per a surfactant molecule in micellar state ($H = H_1 + \beta H_2$) as a fitting parameter, where β is the degree of counterion binding. The axial ratio of the micellar core a_c is determined from m through the following relations:

$$m\nu_c = (4/3)\pi a_c R_c^3, \quad \text{for prolate} \quad (9a)$$

$$= (4/3)\pi a_c^2 R_c^3, \quad \text{for oblate} \quad (9b)$$

On the other hand, the axial ratio of whole micelle a is calculated from m by solving the following simultaneous equations

$$m(\nu_c + \nu_s) = (4/3)\pi(a_cR_c + t)(R_c + t)^2, \quad \text{for prorate} \quad (10a)$$

$$= (4/3)\pi(a_cR_c + t)^2(R_c + t), \quad \text{for oblate} \quad (10b)$$

$$a = (a_cR_c + t)/(R_c + t) \quad (11)$$

where t is the thickness of the shell.

The intermicellar structure factor *S(q)* in eq 1 is a function of the micelle diameter, charge ($m(1 - \beta)$), the number density of micelles (N_p), and the dielectric constant of the solvent. We have calculated *S(q)* by using the rescaled mean spherical approximation (RMSA) proposed by Hayter, Penfold, and Hansen.[25,26] In this model, the micelle is assumed to be a rigid charged sphere of diameter, σ. The σ value for oblate and prolate ellipsoid particle was set equal to that of a sphere of equivalent volume, an average diameter. This method neglects the finite size of the counterions and is approximate in its treatment of double-layer repulsion. Hence, the value of the charge is the apparent charge of the micelle.

Thus, all the parameters needed to calculate *I(q)* are functions of R_c, m, β, and H, which are used as free-fitting parameters in the nonlinear least-squares analysis of the data. In addition to them, a scaling parameter, A, was used as a free-fitting parameter due to uncertainty in calibration for absolute intensity.

TABLE 1: Physical Constants Used in the Analysis of SAXS and SANS Data

moiety	vol/cm^3 mol^{-1} [a]	vol/Å^3[a]	b_{coh}/fm[b]	Z
CF_2	27.0	44.9	17.96	24
CF_3	44.0	73.7	23.61	33
COO^-	22.3	37.0	18.26	23
Cs^+	21.34[c]	35.4[c]	5.42	54
H_2O	18.1	29.9	−1.67	10
D_2O	18.1	29.9	19.15	10

[a] From ref 20 except for Cs^+. [b] From ref 21. [c] From ref 22.

Results

Figures 1 and 2 show observed SAXS and SANS data, respectively, for CsPFO−H_2O solutions at different concentrations and least-squares fits for prolate ellipsoid (Figures 1a and 2a) and oblate ellipsoid (Figures 1b and 2b) models. The fitted parameters are summarized in Table 2. It should be mentioned that the fitted parameters obtained from the SANS data have much larger errors than from the SAXS data. This comes from

TABLE 2: Fitted Parameters for Prolate and Oblate Ellipsoid Models

method	C/mol dm^{-3}	m	β	H	R_c/Å	A
			Prolate Ellipsoid Model			
SANS	0.063	51 (21)	0.53 (0.55)	0 (65)	12.8 (9.3)	0.86 (0.57)
SANS	0.096	58 (10)	0.69 (0.74)	29 (223)	14.2 (8.4)	0.81 (0.31)
SAXS	0.10	69 (2)	0.61 (0.02)	5 (3)	15.5 (0.6)	0.69 (0.03)
SAXS	0.15	81 (2)	0.66 (0.02)	3 (3)	15.8 (0.5)	0.52 (0.02)
SAXS	0.22	94 (2)	0.78 (0.01)	13 (3)	15.2 (0.3)	0.47 (0.02)
SANS	0.31	106 (10)	0.84 (0.20)	19 (77)	15.9 (0.9)	0.71 (0.22)
SANS	0.50	138 (3)	0.86 (0.15)	9 (38)	16.8 (1.0)	0.71 (0.18)
			Oblate Ellipsoid Model			
SANS	0.063	50 (13)	0.61 (0.95)	1 (163)	11.4 (30.0)	0.92 (0.31)
SANS	0.096	58 (12)	0.73 (0.37)	54 (231)	13.6 (13.0)	0.82 (0.47)
SAXS	0.10	70 (2)	0.58 (0.03)	4 (3)	13.4 (0.9)	0.70 (0.02)
SAXS	0.15	82 (2)	0.62 (0.03)	1 (2)	13.5 (0.7)	0.51 (0.02)
SAXS	0.22	100 (2)	0.71 (0.02)	2 (2)	12.7 (0.5)	0.41 (0.02)
SANS	0.31	110 (15)	0.73 (0.37)	0 (31)	14.1 (6.1)	0.60 (0.21)
SANS	0.50	132 (12)	0.85 (0.30)	13 (84)	10.8 (2.6)	0.81 (0.44)

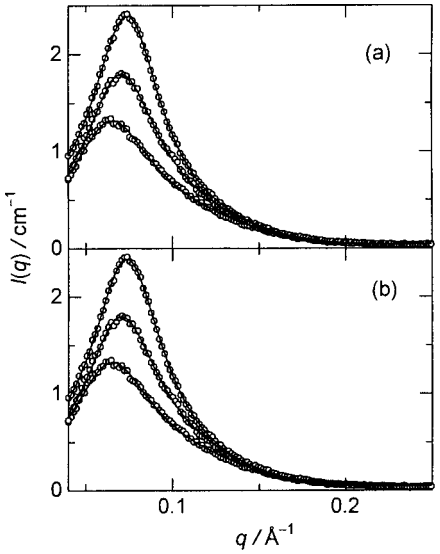

Figure 1. SAXS data and best fits using prolate (a) and oblate (b) ellipsoid models for 0.10, 0.15, and 0.22 M (from the bottom) CsPFO in H_2O.

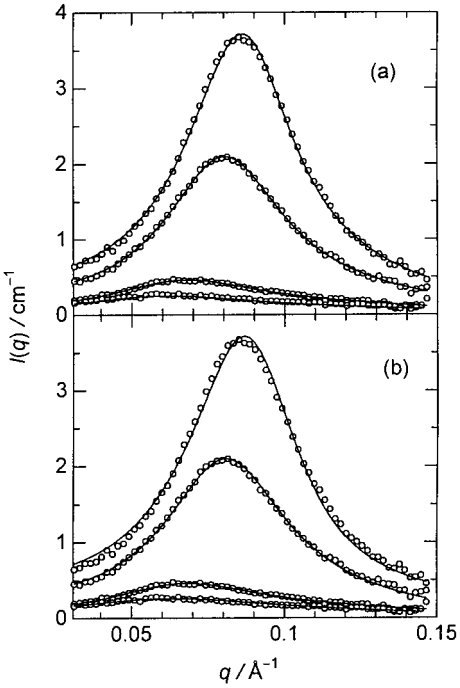

Figure 2. SANS data and best fits using prolate (a) and oblate (b) ellipsoid models for 0.06, 0.10, 0.31, and 0.50 M (from the bottom) CsPFO in H_2O.

the fact that q-range for the SANS measurements is narrower than for the SAXS measurements as can be seen from Figures 1 and 2.

The length of the semiminor axis (R_c) obtained from the SAXS data is shown in Figure 3 as a function of concentration. This figure demonstrates that the R_c values at different concentrations are almost the same within the experimental error. To determine the concentration dependence of the aggregation number (m) and the degree of counterion binding (β), therefore, we fixed R_c to the averaged value obtained from the SAXS data, i.e., 15.3 ± 0.4 and 13.0 ± 0.5 Å for prolate and oblate ellipsoid models, respectively.[27] The fitting curves for these R_c values are almost the same as those in Figures 1 and 2. Table 3 summarizes fitted parameters thus obtained. This table contains also the axial ratio of micelles calculated from the aggregation number (see eq 10).

In Figure 4, the aggregation number m is plotted against $(C - \mathrm{cmc})^{1/2}$. The filled and open symbols correspond to the SAXS and SANS results, respectively. The aggregation numbers obtained by using these two methods fall into the same line. Moreover, both prolate (triangles) and oblate (circles) ellipsoid models give almost the same aggregation number within the experimental errors. Berr and Jones[20] analyzed their SANS data on a sodium perfluorooctanoate (SPFO)−water system using spherical micellar model. Their results are indicated by squares in Figure 4. The extrapolation of m to the cmc for these two systems gives almost the same value (about 20). As the concentration increases, however, the aggregation number of CsPFO micelles increases more rapidly than that of SPFO micelles.

Concentration dependence of β is presented in Figure 5. It can be seen from the figure that the β values of CsPFO are much larger than those of SPFO in the entire concentration range although both systems give rapid increase of β with increasing surfactant concentration.

Figures 6 and 7 show SANS data and best fits for 0.10 and 0.31 M CsPFO solutions, respectively, where the contrast is varied by adding D_2O to H_2O. Although the experimental errors are large except for 100% H_2O and 100% D_2O, the fitted parameters are independent of the mixing ratio, supporting the core−shell model used in our analysis (see Tables 4 and 5).

Discussion

Semiminor Axis of Micellar Core and Extended Length of Fluorocarbon Chain. The observed SAXS and SANS data

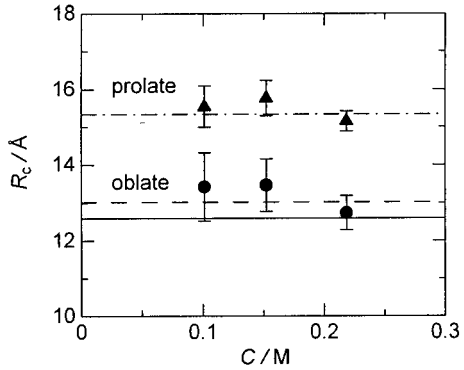

Figure 3. Length of semiminor axis (R_c) obtained from the fitting of SAXS data using prolate (triangles) and oblate (circles) ellipsoid models vs concentration of CsPFO. Dash-dot-line, averaged value for prolate ellipsoid model; dashed line, averaged value for oblate ellipsoid model; solid line, extended length of fluorocarbon chain calculated from eq 13.

TABLE 3: Fitted Parameters for Prolate and Oblate Ellipsoid Models with Fixed R_c

method	C/mol dm^{-3}	m	β	H	A	a
Prolate Ellipsoid Model (R_c = 15.3 Å)						
SANS	0.063	52 (9)	0.60 (0.23)	0 (37)	0.85 (0.20)	1.17
SANS	0.096	58 (8)	0.72 (0.43)	48 (228)	0.81 (0.35)	1.17
SAXS	0.10	69 (2)	0.61 (0.02)	6 (3)	0.70 (0.02)	1.46
SAXS	0.15	80 (1)	0.67 (0.02)	5 (2)	0.54 (0.01)	1.66
SAXS	0.22	95 (1)	0.78 (0.01)	11 (1)	0.46 (0.01)	1.84
SANS	0.31	105 (1)	0.84 (0.04)	21 (13)	0.73 (0.04)	1.88
SANS	0.50	141 (3)	0.88 (0.03)	13 (2)	0.80 (0.01)	2.52
Oblate Ellipsoid Model (R_c = 13.0 Å)						
SANS	0.063	51 (9)	0.61 (0.24)	0 (40)	0.86 (0.21)	1.35
SANS	0.096	58 (14)	0.71 (0.65)	40 (308)	0.81 (0.54)	1.24
SAXS	0.10	69 (2)	0.58 (0.03)	5 (3)	0.70 (0.02)	1.49
SAXS	0.15	82 (2)	0.62 (0.02)	2 (2)	0.54 (0.01)	1.65
SAXS	0.22	101 (1)	0.71 (0.02)	1 (2)	0.46 (0.01)	1.84
SANS	0.31	108 (6)	0.75 (0.19)	3 (21)	0.64 (0.07)	1.83
SANS	0.50	134 (9)	0.86 (0.14)	11 (41)	0.72 (0.15)	1.83

TABLE 4: Fitted Parameters for Prolate and Oblate Ellipsoid Models with Fixed R_c for 0.10 M CsPFO Solutions of Different D_2O/H_2O Ratios

% D_2O	m	β	H	A
Prolate Ellipsoid Model (R_c = 15.3 Å)				
0	54 (9)	0.67 (0.48)	37 (183)	0.75 (0.32)
18	66 (24)	0.73 (1.05)	36 (469)	0.39 (0.42)
38	66 (27)	0.61 (3.43)	42 (923)	0.43 (0.81)
100	59 (1)	0.85 (0.04)	109 (8)	0.94 (0.02)
Oblate Ellipsoid Model (R_c = 13.0 Å)				
0	54 (8)	0.67 (0.45)	34 (161)	0.76 (0.30)
18	67 (28)	0.71 (1.00)	28 (389)	0.38 (0.40)
38	66 (27)	0.62 (3.00)	43 (878)	0.43 (0.77)
100	58 (4)	0.73 (0.17)	54 (97)	0.91 (0.17)

can be fitted to both prolate and oblate ellipsoid models. As can be seen from Figure 3, however, the R_c values obtained for the prolate ellipsoid is much higher than those for the oblate ellipsoid. So we compare these values with the extended length of a fluorocarbon chain (l_{ext}) obtained from the following equation originally proposed for a hydrocarbon chain[28]

$$l_{ext} = r_{CF_3} + d_{C-C}(n_c' - 1) + r_{CF_2} \quad (12)$$

where r_{CF_3} and r_{CF_2} are the radius of the terminal perfluoromethyl and α-perfluoromethylene groups, respectively, determined from their volumes (v_{CF_3} and v_{CF_2}, respectively) in Table 1, d_{C-C} is the distance between adjacent carbons in the direction parallel to the chain axis,[29] and n_c' is the number of carbon in the hydrophobic chain. Inserting the values r_{CF_3} = 2.60 Å, r_{CF_2} = 2.20 Å, d_{C-C} = 1.294 Å, we obtain

$$l_{ext}/\text{Å} = 3.51 + 1.294n_c' \quad (13)$$

For n_c' = 7, l_{ext} is calculated to be 12.6 Å which is indicated by the solid line in Figure 3. Clearly, the R_c value obtained for the prolate ellipsoid is much larger than l_{ext}, corresponding to the unrealistic situation that there exists a space that is not filled with fluorocarbons. On the other hand, the R_c value for the oblate ellipsoid model, 13.0 Å, is close to the l_{ext} value. These results suggest that the oblate ellipsoid is the more preferable model for the CsPFO micelles than the prolate ellipsoid model.

TABLE 5: Fitted Parameters for Prolate and Oblate Ellipsoid Models with Fixed R_c for 0.31 M CsPFO Solutions of Different D_2O/H_2O Ratios

% D_2O	m	β	H	A
Prolate Ellipsoid Model (R_c = 15.3 Å)				
0	105 (1)	0.84 (0.04)	21 (13)	0.73 (0.04)
18	108 (5)	0.81 (0.11)	9 (25)	0.84 (0.10)
36	111 (3)	0.85 (0.09)	21 (25)	0.99 (0.07)
Oblate Ellipsoid Model (R_c = 13.0 Å)				
0	108 (6)	0.75 (0.19)	3 (21)	0.64 (0.07)
18	109 (10)	0.76 (0.32)	1 (33)	0.75 (0.14)
36	111 (12)	0.85 (0.33)	21 (135)	0.92 (0.40)

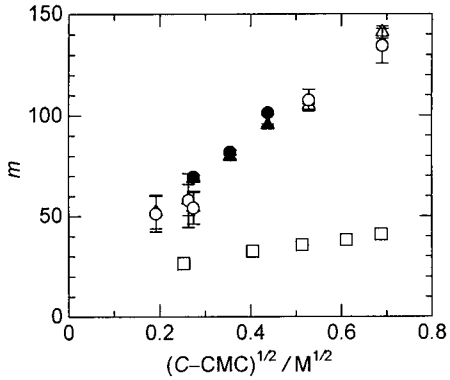

Figure 4. Aggregation number (m) vs square root of the surfactant concentration forming micelles obtained from the fitting of SAXS (filled symbols) and SANS (open symbols) data using prolate (triangles) and oblate (circles) ellipsoid models with fixed semiminor axis. The squares indicate the values obtained for sodium perfluorooctanoate using spherical micellar model reported by Berr and Jones.[20]

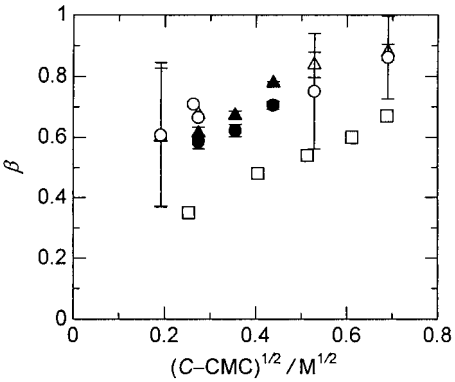

Figure 5. Degree of counterion binding β vs square root of the surfactant concentration forming micelles obtained from the fitting of SAXS (filled symbols) and SANS (open symbols) data using prolate (triangles) and oblate (circles) ellipsoid models with fixed semiminor axis. The squares indicate the values obtained for sodium perfluorooctanoate using spherical micellar model reported by Berr and Jones.[20]

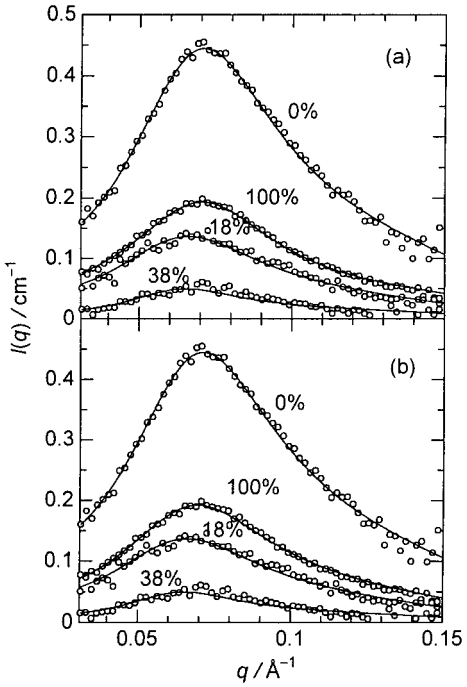

Figure 6. SANS data and best fits using prolate (a) and oblate (b) ellipsoid models for 0.10 M CsPFO solutions of different D_2O/H_2O ratios. The numbers in the figure indicate mole percent of D_2O in the solvent.

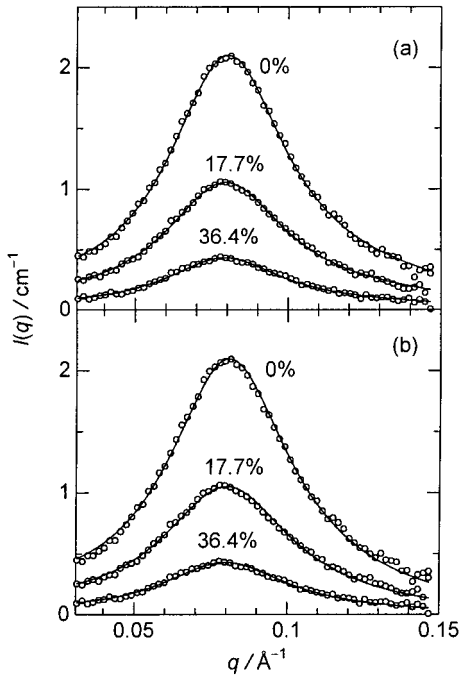

Figure 7. SANS data and best fits using prolate (a) and oblate (b) ellipsoid models for 0.31 M CsPFO solutions of different D_2O/H_2O ratios. The numbers in the figure indicate mole percent of D_2O in the solvent.

Comparison with the Studies of Boden *et al.* As described in the Introduction, Boden *et al.* established the existence of the discotic nematic phase in the CsPFO−water system. They obtained the aggregation number both in the nematic phase and in the isotropic phase. In the latter case, they assumed that the observed SAXS peak corresponds to the scattering from the (111) planes of a fcc lattice. To check the validity of this assumption, we compare the aggregation number obtained from this method with the present results in the following manner.

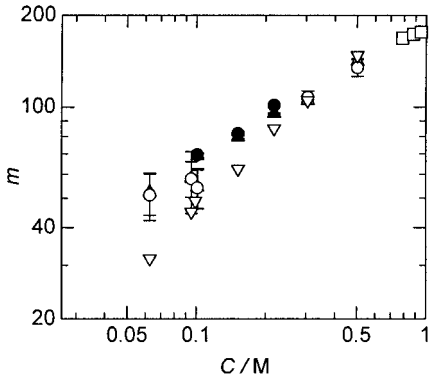

Figure 8. Comparison between the aggregation number obtained from the fitting of scattering curves (the symbols are the same as in Figure 4 except for squares) and that obtained from the position of the scattering peak assuming a fcc lattice using the data of authors' (inverted triangles) and Boden *et al.*[7] (squares).

The lattice constant of the fcc lattice (a_{fcc}) is related to the distance between the (111) planes (d_{111}) through the equation

$$a_{fcc} = 3^{1/2} d_{111} \tag{14}$$

On the other hand, the number density of micelles can be written as

$$N_p = 4/{a_{fcc}}^3 = 4/(3^{1/2} d_{111})^3 \tag{15}$$

If the concentration of surfactants forming micelles can be approximated by $C -$ cmc, the following relation holds between the aggregation number m and the surfactant concentration C.

$$C - \text{cmc} = mN_p/N_A \tag{16}$$

where N_A is an Avogadro's number. Using eqs 15 and 16 together with the Bragg equation, we obtain

$$m = (1/4)(2\pi 3^{1/2}/q_{max})^3 N_A(C-\text{cmc}) \tag{17}$$

where q_{max} is the q value at the scattering peak. In Figure 8, we compare the aggregation number obtained from the observed q_{max} using eq 17 with that obtained from the fitting of the scattering curve. The agreement is quite good in the higher concentration range, suggesting that eq 17 holds approximately at least near the nematic phase. As the concentration decreases, however, the m value obtained from eq 17 becomes smaller than that obtained from the curve fitting.

Figure 8 presents also the aggregation number reported by Boden *et al.* in the isotropic phase. As expected from the foregoing results, there is no discontinuity between these two sets of data, indicating that the aggregation number increases monotonously as the concentration increases up to about 1 M, in the vicinity of the nematic phase. These results are consistent with the bidimensional growth of CsPFO micelles. As the building unit of the nematic phase is a disklike micelle, it may be natural consequence that micelles in the dilute region are disklike. It should be emphasized, however, that no one has so far reported experimental data indicating the existence of the disklike micelles in the concentration range much lower than the nematic phase (see later).

Comparison with Sodium Salts and Ammonium Salts of Perfluorooctanoic Acid. The aggregation number of spherical

micelles can be estimated from the volume of fluorocarbon part of a surfactant molecule (v_{fc}) and the radius of sphere (r) as

$$m_{sp} = (4/3)(r^3/v_{fc}) \quad (18)$$

$$v_{fc} = v_{CF_3} + (n_c' - 1)v_{CF_2} \quad (19)$$

Using the values of v_{CF_3} and v_{CF_2} in Table 1, m_{sp} is calculated to be 24.4, 26.8, and 43.7 for $r = 12.6$ Å (extended length of the hydrophobic chain calculated from eq 13), 13.0 Å (the semiminor axis R_c obtained from the fits for oblate ellipsoid model), and 15.3 Å (the semiminor axis R_c obtained from the fits for prolate ellipsoid model), respectively. If the shape of micelles formed at the cmc is close to sphere, the value $m_{sp} = 43.7$ is too large compared to the observed value at the cmc, about 20. This indicates that the semiminor axis obtained for the prolate ellipsoid model is again too long. In other words, the prolate ellipsoid model may be inadequate for the CsPFO system.

The aggregation numbers of CsPFO and SPFO[20] are almost the same at the cmc. However, the CsPFO micelles grow more rapidly than the SPFO micelles as the surfactant concentration increases. This may be a result of the fact that the cesium ion is attached to the micellar surface more strongly than the sodium ion. In fact, the degree of counterion binding β for the CsPFO system increases up to about 0.9 as the surfactant concentration increases up to 0.5 M. On the other hand, the β value for the SPFO system is less than 0.6 even at 0.5 M (see Figure 5).

Burkitt *et al.*[30] measured SANS for 0.12 M ammonium perfluorooctanoate (APFO) in NH_4Cl:NH_4OH buffer solutions at pH = 8.8 and an ionic strength of 0.1. They showed that the observed scattering curves can be reproduced by the form factor for cylinders with radius of 10 Å and length of 48 Å. Very recently, Kunze *et al.*[31] have studied the APFO in 0.5 M NH_4Cl by SANS and SAXS. They have analyzed their data using the form factor for cylinders with core and shell. According to their results, all APFO is present in rodlike micelles with radius 16 Å and length in excess of 300 Å when the weight fraction of APFO (w) is less than 0.05. At $w = 0.25$, on the other hand, only disklike micelles occur with thickness 32 Å and radius 26 Å. As the thickness of the shell was fixed to 4 Å, both the core radius of rodlike micelles and half the core thickness of the disklike micelles are 12 Å which is close to the extended length of a fluorocarbon chain, 12.6 Å. In the analyses of Burkitt *et al.* and Kunze *et al.*, the structure factor *S(q)* is fixed to unity as the Coulombic forces between micelles are reduced by the addition of salt.

These systems differ from our system as to the counterion and the ionic strength. In our system, there is no additional salt and so there exists still strong electrostatic repulsion between micelles even in the dilute region. This may stabilize the disklike micelles because the excluded volume interactions between them are smaller than those between rodlike micelles. To confirm this prediction, measurements of SANS on CsPFO solutions containing cesium chloride are currently under way and will be reported elsewhere.

References and Notes

(1) For example: Ben-Shaul, A.; Gelbert, W. M. In *Micelles, Membranes, Microemulsions, and Monolayers;* Gelbert, W. M., Ben-Shaul, A., Roux, D., Eds.; Springer-Verlag: New York, 1994.
(2) Israelachvili, Y. N.; Mitchell, D. J.; Ninham, B. W. *J. Chem. Soc., Faraday Trans. 2* **1976**, *72*, 1525.
(3) Lin, T-L.; Liu, C-C.; Roberts, M. F.; Chen, S-H. *J. Phys. Chem.* **1991**, *95*, 6020.
(4) Boden, N.; Jackson, P. H.; McMullen, K.; Holmes, M. C. *Chem. Phys. Lett.* **1979**, *65*, 476.
(5) Boden, N.; Corne, S. A.; Jolley, K. W. *J. Phys. Chem.* **1987**, *91*, 4092.
(6) Boden, N.; Corne, S. A.; Holmes, M. C.; Jackson, P. H.; Parker, D. *J. Phys.* **1986**, *47*, 2135.
(7) Holmes, M. C.; Reynolds, D. J.; Boden, N. *J. Phys. Chem.* **1987**, *91*, 5257.
(8) Holmes, M. C.; Reynolds, D. J.; Boden, N. *Mol. Cryst. Liq. Cryst.* **1987**, *146*, 377.
(9) Boden, N.; Jolley, K. W.; Smith, M. H. *J. Phys. Chem.* **1993**, *97*, 7678.
(10) Leaver, M. S.; Holmes, M. C. *J. Phys. 2 (Fr.)* **1993**, *3*, 105.
(11) Holmes, M. C.; Smith, A. M.; Leaver, M. S. *J. Phys. 2 (Fr.)* **1993**, *3*, 1357.
(12) Boden, N. In *Micelles, membranes, Microemulsions, and Monolayers;* Gelbert, W. M., Ben-Shaul, A., Roux, D., Eds.; Springer-Verlag: New York, 1994.
(13) Holmes, M. C.; Leaver, M. S.; Smith, A. M. *Langmuir* **1995**, *11*, 356.
(14) Iijima, H.; Kato, T.; Seimiya, T.; Yoshida, H.; Imai, M. *Prog. Colloid Polym. Sci.*, in press.
(15) Iijima, H.; Koyama, S.; Fujio, K.; Uzu, Y., to be published.
(16) Kato, S.; Harada, S.; Nakashima, N.; Nomura, H. *J. Colloid Interface Sci.* **1992**, *150*, 305.
(17) Yoshida, H.; Kinoshita, R.; Teramoto, Y. *Thermochim. Acta* **1995**, *264*, 173.
(18) Kotlarchk, M.; Chen, S-H. *J. Chem. Phys.* **1983**, *79*, 2461.
(19) Chen, S-H.; Lin, T-L. In *Methods of Experimental Physics*; Academic Press: New York, 1987; Vol. 23, Part B.
(20) Berr, S. S.; Jones, R. R. M. *J. Phys. Chem.* **1989**, *93*, 2555.
(21) Sears, V. F. In *Methods of Experimental Physic*; Academic Press: New York, 1987; Vol. 23, part A.
(22) Millero, F. J. *Chem. Rev.* **1971**, *71*, 147.
(23) The change in the monomer concentration does not affect the results very much except for the degree of counter ion binding.[24]
(24) Iijima, H.; Kato, T.; H.; Imai, M.; Soderman, O., to be published.
(25) Hayter, J. B.; Penfold, J. *Mol. Phys.* **1981**, *42*, 109.
(26) Hansen, J-P.; Hayter, J. B. *Mol. Phys.* **1982**, *46*, 651.
(27) The R_c values obtained from the SANS data were not used in this average process as the errors are extremely large.
(28) Berr, S. S.; Coleman, M. J.; Jones, R. R. M.; Johnson, J. S., Jr. *J. Phys. Chem.* **1986**, *90*, 6492.
(29) Bunn, C. W.; Howells, E. R. *Nature* **1954**, *174*, 549.
(30) Burkitt, S. J.; Ottewill, R. H.; Hayter, J. B.; Ingram, B. T. *Colloid Polym. Sci.* **1987**, *265*, 619.
(31) Kunze, B.; Kalus, J.; Boden, N.; Brandao, M. S. B. *Physica B* **1997**, *234*, 351.